pH-Controlled Assembly and Properties of LbL Membranes from Branched Conjugated Poly(alkoxythiophene sulfonate) and Various Polycations

Veronika Kozlovskaya,[†] Eugenia Kharlampieva,[†] Keith Jones,[†] Zhiqun Lin,[‡] and Vladimir V. Tsukruk*,[†]

[†]*School of Materials Science and Engineering and School of Polymer, Textile and Fiber Engineering, Georgia Institute of Technology, Atlanta, Georgia 30332 and* [‡]*School of Materials Science and Engineering, Iowa State University, Ames, Iowa 50011*

We report on multilayer layer-by-layer (LbL) films of the conjugated polymer sodium poly[2-(3-thienyl)ethyloxy-4-butylsulfonate] (PTH) assembled with polycations: poly(diallyldimethylammonium chloride) (PDDA), 20% quaternized poly(N-ethyl-4-vinylpyridinium bromide) (Q20), poly(ethylene imine) (PEI), and poly(allylamine hydrochloride) (PAH). These films were prepared through spin-assisted LbL assembly under various pH conditions. We demonstrated a crucial role of the deposition pH in formation of PTH/polycation films and showed that decrease in the deposition pH from 7.5 to 2.5 limits the PTH multilayer formation to Q20/PTH and PDDA/PTH films due to reduced charge density in the poly(thiophene) chains. We show that optical and surface properties of the resulting PTH/polycation films can be tuned by varying a polycation component and/or by varying the deposition pH. The fluorescence properties of the Q20/PTH, PEI/PTH, and PDDA/PTH films are pH-dependent, and the films exhibit the drastic changes in photoluminescent intensity when transferred into solutions with different pH values, which may find useful in optical sensing applications.

Introduction

Chemical sensing with optical readout is considered to be promising for facile colorimetric-based detection scheme.[1−3] Ultrathin films with responsive optical properties have been demonstrated to be of a potential use for this field due to multifunctional physicochemical properties, tunability of the composition, and triggered response to external stimuli.[4−8] It is worth noting that for practical applications it is important to be able to fabricate films which can be later transferred to various microfabricated substrates of actual devices.[9,10] This ability is important as such free-standing films possess a faster response and permeability due to their short diffusion-limited path for incoming analytes as well as versatility in integration with various microfabricated substrates.

Conjugated polymers comprise a class of functional materials with unique conducting and optical properties such as easily quenchable photoluminescence which can be explored for bio-

and chemo-sensing applications.[11−13] Controlling optical properties has been shown possible through changes of the geometric conformation of the conjugated polymers via electrostatically combining the conjugated polyelectrolyte with a charged surfactant, thereby resulting in enhanced fluorescence of such complexes.[14] The presence of charged compounds has been demonstrated to affect fluorescence of the conjugated polyelectrolytes in solutions.[15] However, loss of fluorescence or significant changes in optical spectra has been observed when some conjugated polymers were transferred from solutions to solid substrates due to crystallization, aggregation, or interaction with solid substrates.[16,17]

Solubility of poly(thiophene)s in water is considered an important property for future applications of these materials, and water-soluble poly(thiophene)s have recently received much attention due to their potential applications in bio- and chemosensing.[18−22] Introducing various modified side chains to the conjugated backbones of the poly(thiophenes) can result in new materials with useful functionalities.[23] For example, a carboxy-functionalized poly(thiophene) has been utilized as a sensor for

*To whom correspondence should be addressed. E-mail: Vladimir@mse.gatech.edu.

(1) Lee, J.; Hernandez, P.; Lee, J.; Govorov, A.; Kotov, N. A. *Nat. Mater.* **2007**, *6*, 291–295.
(2) Goicoechea, J.; Arregui, F. J.; Corres, J. M.; Matias, I. R. *J. Sens.* **2008**, DOI: 10.1155/2008/142854.
(3) Kozlovskaya, V.; Kharlampieva, E.; Khanal, B. P.; Manna, P.; Zubarev, E. R.; Tsukruk, V. V. *Chem. Mater.* **2008**, *20*, 7474–7485.
(4) Tsukruk, V. V. *Prog. Polym. Sci.* **1997**, *22*, 247–311.
(5) Sidorenko, A.; Krupenkin, T.; Taylor, A.; Fratzl, P.; Aizenberg, J. *Science* **2007**, *315*, 487–490.
(6) Jiang, C.; Tsukruk, V. V. *Soft Matter* **2005**, *1*, 334–337.
(7) Tokarev, I.; Tokareva, I.; Minko, S. *Adv. Mater.* **2008**, *20*, 2730–2734.
(8) Luzinov, I.; Minko, S.; Tsukruk, V. V. *Prog. Polym. Sci.* **2004**, *29*, 635–698.
(9) Jiang, C.; Tsukruk, V. V. *Adv. Mater.* **2006**, *18*, 829–840.
(10) Miller, L. L.; Zhong, C. J.; Kasai, P. *J. Am. Chem. Soc.* **1993**, *115*, 5982–5990.
(11) Achyuthan, K. E.; Bergstedt, T. S.; Chen, L.; Jones, R. M.; Kumaraswamy, S.; Kushon, S. A.; Ley, K. D.; Lu, L.; McBranch, D.; Mukundan, H.; Rininsland, F.; Shi, X.; Xia, W.; Whitten, D. G. *J. Mater. Chem.* **2005**, *15*, 2648–2656.
(12) Nilsson, K. P. R.; Inganäs, O. *Nat. Mater.* **2003**, *2*, 419–424.
(13) He, F.; Tang, Y. L.; Wang, S.; Li, Y. L.; Zhu, D. B. *J. Am. Chem. Soc.* **2005**, *127*, 12343–12346.

(14) Chen, L.; Xu, S.; McBranch, D.; Whitten, D. *J. Am. Chem. Soc.* **2000**, *122*, 9302–9303.
(15) Dwight, S. J.; Gaylord, B. S.; Hong, J. W.; Bazan, G. C. *J. Am. Chem. Soc.* **2004**, *126*, 16850–16859.
(16) Jones, R. M.; Lu, L.; Helgeson, R.; Bergstedt, T. S.; McBranch, D. W.; Whitten, D. G. *Proc. Natl. Acad. Sci. U.S.A.* **2001**, *98*, 14769–14772.
(17) Gunawidjaja, R.; Luponosov, Y. N.; Huang, F.; Ponomarenko, S. A.; Muzafarov, A. M.; Tsukruk, V. V. *Langmuir* **2009**, *19*, 9270–9284.
(18) Gaylord, B. S.; Heeger, A. J.; Bazan, G. C. *Proc. Natl. Acad. Sci. U.S.A.* **2002**, *99*, 10954–10957.
(19) Pinto, M. R.; Schanze, K. S. *Proc. Natl. Acad. Sci. U.S.A.* **2004**, *101*, 7505–7510.
(20) Tong, H.; Wang, L.; Wang, J.; Jing, X.; Wang, F. *Macromolecules* **2002**, *35*, 7169–7171.
(21) Liang, Z.; Dzienis, K. L.; Xu, J.; Wang, Q. *Adv. Funct. Mater.* **2006**, *16*, 542548.
(22) Kim, H.-C.; Lee, S.-K.; Jeon, W. B.; Lyu, H.-K.; Lee, S. W.; Jeong, S. W. *Ultramicroscopy* **2008**, *108*, 1379–1383.
(23) Cagnoli, R.; Lanzi, M.; Libertini, E.; Mucci, A.; Paganin, L.; Parenti, F.; Preti, L.; Schenetti, L. *Macromolecules* **2008**, *41*, 3785–3792.

amine-functionalized compounds where intra- or interchain conformational changes induced by interactions with analytes produced specific optical fingerprints.[24] It has been shown that the fluorescence of poly(thiophene-3-yl-acetic acid 8-quinolinyl ester) can be quenched by the addition of HCl, which can be recovered by the addition of equivalent amounts of alkali. The fluorescence of the polymer was also quenched by copper, cadmium, and lead metal ions with the sensitivity to their concentrations.[25] Self-quenching of the thymine moiety-containing poly(thiophene) has been explored as a selective chemosensor for mercury ions with 60% of fluorescence quenching efficiencies.[26] Attachment of ionic, i.e., sulfonate groups, allowed formation of counterions in the close proximity of the backbone leading to self-acid-doped conducting polymers.[27] However, the presence of polar carboxylic side groups in poly(thiophene-3-acetic acid) is related to lower electron transport in the polymer due to their polarity and close proximity to the conjugate backbone.[28]

Sodium poly[2-(3-thienyl)ethyloxy-4-butylsulfonate] (PTH) with branched backbones and high concentration of ionic side groups is a unique water-soluble polymer whose solubility in water depends on its molecular weight.[29] It has been shown that PTH with more than 3500 monomer units possesses good solubility in aqueous solutions, and its absorption and fluorescence maxima shift to longer wavelengths with the increased conjugation length.[30] The photoluminescence quenching of this polymer was also reported due to changes in the molecular weight or ionic strength of the polymer solutions.[30] Moreover, instability of the PTH solutions was reported in the presence of salt ions when thermodynamically favored formation of micellar-like structures occurred over a period of several days in presence of mono- and/or divalent ions.

Modern sensing applications require a new design of responsive functional coatings capable of changing their properties in a controlled way under external stimuli. Chemical grafting and SAM approaches are both significantly limited by specific chemistry of substrates. While grafting approaches require surface functionalization with specific initiators capable of supporting polymerization or grafting chemical reactions, the SAM approach is even more restrictive due to requirement of thiol−metal bonds between organic molecules and surfaces, which limits application of these methods to particular surfaces.

Layer-by-layer (LbL) assembly is a versatile way to create ultrathin polymer membranes with controlled properties.[31,32] Layers of a polyanion and a polycation can be stepwise deposited onto a surface through conventional (dipping) and spin-assisted (SA) assembly, thereby producing robust LbL films. The LbL assembly has been applied to construct a wide range of ultrathin films from conjugated polymers.[33−35] Encapsulation of fluorescent polyelectrolytes or inorganic components in LbL films can critically affect overall optical properties leading to either preservation, alternation, or enhancement of initial optical properties as has been demonstrated in a number of cases.[36,37]

The SA-LbL assembly[38,39] offers the advantages over the conventional assembly of much shorter fabrication times and firm control over the bilayer thickness and thus is considered to be more "technologically friendly". Moreover, the resulting SA-LbL films with highly stratified inner organization show enhanced robustness and mechanical properties.[40,41] Furthermore, these robust ultrathin flexible films have shown extraordinary sensitivity and dynamic range in the freely suspended state, with a potential application as a new generation of pressure and temperature sensor arrays. Finally, SA-LbL offers the incorporation of nonpolar hydrophobic moieties and the layering of complex biological materials, which would be challenging with conventional LbL assembly. Responsive properties of thin LbL films are relevant for biotechnology and biomedicine as these films can follow the dynamic changes in living systems acting as reporters of pH or environment changes in the culturing medium. In our recent studies, we have applied SA-LbL to fabricate planar and sculptured ultrathin films from conjugated polymers which showed exemplary mechanical stability in free-standing state and robust fluorescent properties.[42−44]

In this work, we employ the SA-LbL assembly to the branched conjugated polyelectrolyte, PTH, in conjunction with weak and strong polycations under various pH conditions to control optical properties of such films. We found that deposition pH plays a crucial role in the SA-LbL assembly of PTH and that all four polycations used in this work, namely, (poly(diallyldimethylammonium chloride) (PDDA), 20% quaternized poly(N-ethyl-4-vinylpyridinium bromide) (Q20), poly(ethylene imine) (PEI), and poly(allylamine hydrochloride) (PAH), produce stable LbL films with bright photoluminescence at high pH. In contrast with previous studies, we focused on how optical properties and morphology of the produced PTH/polycation films can be controlled by varying a nature of polycation component and/or the deposition pH for the same PTH/polycation system. We demonstrate that the Q20/PTH, PEI/PTH, and PDDA/PTH films show a very high photoluminescence when deposited from solution with pH 7.5 but drastically decreased intensity at pH 2.5. We observe that such abrupt change in fluorescence is attributed to a pH-triggered self-quenching of PTH in the film triggered by the selective release of the polycation component from the PTH/polycation films. In the case of Q20/PTH and PDDA/PTH films assembled at pH = 4, the fluorescence can be recovered upon pH changes to higher pH values.

(24) Maynor, M. S.; Nelson, T. L.; O'Sullivan, C.; Lavigne, J. J. *Org. Lett.* **2007**, *9*, 3217–3220.

(25) Maiti, J.; Pokhrel, B.; Boruah, R.; Dolui, S. K. *Sens. Actuators, B* **2009**, *141*, 447–451.

(26) Tang, Y.; He, F.; Yu, M.; Feng, F.; An, L.; Sun, H.; Wang, S.; Li, Y.; Zhu, D. *Macromol. Rapid Commun.* **2006**, *27*, 389–392.

(27) Chayer, M.; Faïd, K.; Leclerc, M. *Chem. Mater.* **1997**, *9*, 2902–2905.

(28) Zhang, F.; Srinivasan, M. P. *Mater. Chem. Phys.* **2008**, *112*, 223–225.

(29) López Cabarcos, E.; Carter, S. A. *Macromolecules* **2005**, *38*, 4409–4415.

(30) López Cabarcos, E.; Carter, S. A. *Macromolecules* **2005**, *38*, 10537–10541.

(31) *Multilayer Thin Films: Sequential Assembly of Nanocomposite Materials*; Decher, G., Schlenoff, J. B., Eds.; Wiley-VCH: Weinheim, Germany, 2002.

(32) Tang, Z.; Kotov, N. A.; Magonov, S.; Ozturk, B. *Nat. Mater.* **2003**, *2*, 413–418.

(33) DeLongchamp, D. M.; Kastantin, M.; Hammond, P. T. *Chem. Mater.* **2003**, *15*, 1575–1586.

(34) DeLongchamp, D. M.; Hammond, P. T. *Chem. Mater.* **2004**, *16*, 4799–4805.

(35) (a) Ferreira, M.; Rubner, M. F. *Macromolecules* **1995**, *28*, 7107–7114. (b) Ferreira, M.; Onitsuka, O.; Stockton, W. B.; Rubner, M. F. *ACS Symp. Ser.* **1997**, *672*, 437–444.

(36) Zimnitsky, D.; Jiang, C.; Xu, J.; Lin, Z.; Tsukruk, V. V. *Langmuir* **2007**, *23*, 4509–4515.

(37) Zimnitsky, D.; Jiang, C.; Xu, J.; Lin, Z.; Zhang, L.; Tsukruk, V. V. *Langmuir* **2007**, *23*, 10176–10183.

(38) Cho, J.; Char, K.; Hong, J.; Lee, K. *Adv. Mater.* **2001**, *13*, 1076–1078.

(39) Chiarelli, P. A.; Johal, M. S.; Casson, J. L.; Roberts, J. B.; Robinson, J. M.; Wang, H.-L. *Adv. Mater.* **2001**, *13*, 1167–1171.

(40) Jiang, C.; Markutsya, S.; Pikus, Y.; Tsukruk, V. V. *Nat. Mater.* **2004**, *3*, 721–728.

(41) Kharlampieva, E.; Kozlovskaya, V.; Chan, J.; Ankner, J. F.; Tsukruk, V. V. *Langmuir* **2009**, *25*, 14017−14024.

(42) Lin, Y. H.; Jiang, C.; Xu, J.; Lin, Z.; Tsukruk, V. V. *Soft Matter* **2007**, *3*, 432–436.

(43) Singamaneni, S.; Jiang, C.; Merrick, E.; Kommireddy, D.; Tsukruk, V. V. *J. Macromol. Sci., Part B: Phys.* **2007**, *46*, 7–19.

(44) Lin, Y. H.; Jiang, C.; Xu, J.; Lin, Z.; Tsukruk, V. V. *Adv. Mater.* **2007**, *19*, 3827–3832.

Experimental Section

Materials. PTH (M_w = 1 000 000) was purchased from American Dye Source (Canada); poly(allylamine hydrochloride) (PAH, M_w = 60 000), poly(diallyldimethylammonium chloride) (PDDA, M_w = 150 000), poly(4-vinylpyridine) (P4VP, M_w = 200 000), hydrochloric acid (HCl), and sodium hydroxide (NaOH) were purchased from Sigma-Aldrich. Poly(ethylene imine) (PEI, branched with M_w = 70 000) was obtained from Polysciences Inc. 1.0 M TRIS buffer was used for solution preparation and was received from VWR International. All chemicals were used as received. Poly(*N*-ethyl-4-vinylpyridinium bromide) with 20% quaternized units (Q20) was synthesized as described elsewhere.[45] Nanopure filtered water with a resistivity 18.2 MΩ·cm was used in all experiments. Quartz fused slides (Alfa Aesar) and single-side polished silicon wafers of the {100} orientation (Semiconductor processing Co.) were cut to a typical size of 10 × 20 mm and cleaned in a piranha solution as described elsewhere.[46] Different pH values of buffer solutions were achieved through adjustment by aqueous 0.01 M HCl or 0.01 M NaOH solutions.

SA-LbL Assembly of PTH/Polycation Films. SA-LbL films of (PTH/polycation)$_n$ were deposited through the SA-LbL method as reported earlier[47] on the quartz microslides or silicon wafers from 0.2 mg/mL aqueous polymer solutions at pH = 7.5, 4, or 2.5. After pH adjustment, all polymer solutions were filtered prior to the assembly process using Acrodisc syringe filters with 0.2 μm nylon membrane (Life Sciences). Specifically, PTH and four polycations were dissolved in 0.01 M TRIS buffer, and pH of the resulting solutions was adjusted to pH = 2.5, 4, and 7.5 using 0.01 M HCl and 0.01 M NaOH solutions. Alternating layers of the PTH and a polycation were deposited by spinning at 4000 rpm up to a total of 20 bilayers. Two rinsing steps were performed in 0.01 M TRIS buffer with the appropriate pH in between each layer to remove excess of polymers. In case when enhanced adsorption of the polymers to surfaces of silicon wafers or quartz slides was needed at a certain pH, three bilayers of PAH (0.2 mg/mL aqueous solution) and poly(styrenesulfonate) (PSS) (0.2 mg/mL aqueous solution) were deposited as primary layers.

UV−Visible Spectroscopy (UV−vis). UV−vis spectra of the films were recorded using a UV-2450 spectrophotometer (Shimadzu). Measurements of the polymer solutions were taken in 1.5 mL semi-microplastic cuvettes (PlastiBrand, Germany) and were done on surface-attached films on quartz slides.

Fluorescence Spectroscopy (FL). Fluorescence spectra were recorded on a RF-5301PC spectrofluorophotometer (Shimadzu). Measurements were taken in four-sided clear 3 mL plastic cuvettes (PlastiBrand, Germany) or on quartz slides.

Atomic Force Microscopy (AFM). Surface morphology of the films was examined using AFM. AFM images were collected using a Dimension 3000 microscope in the "light" tapping mode according to the established procedure.[48] For film thickness measurements, the scratch on the film was made by a thin syringe needle, and the scratched area was scanned and the image was analyzed with Nanoscope software.

Ellipsometry Measurements. Film assembly under different pH conditions as well as the film thickness before and after exposure of the SA-LbL assembled films to different pH values were determined using a M-2000U spectroscopic ellipsometer (Woollam). Prior to the measurements, samples were dried with a stream of nitrogen.

Attenuated Total Reflection−Fourier Transform Infrared Spectroscopy (ATR-FTIR). In situ ATR-FTIR during

(45) Kozlovskaya, V.; Kharlampieva, V.; Mansfield, M. L.; Sukhishvili, S. A. *Chem. Mater.* **2006**, *18*, 328–336.
(46) Tsukruk, V. V.; Bliznyuk, V. N. *Langmuir* **1998**, *14*, 446–455.
(47) Jiang, C.; Markutsya, S.; Tsukruk, V. V. *Adv. Mater.* **2004**, *16*, 157–161.
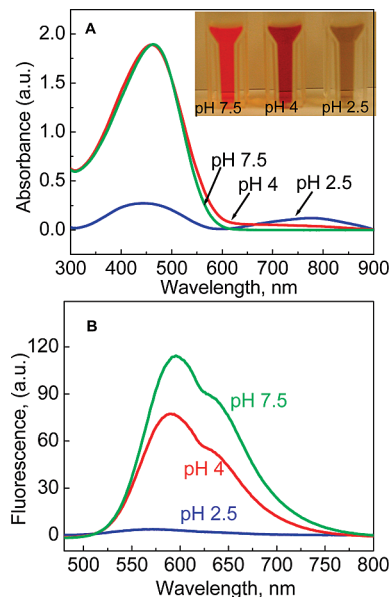(48) Tsukruk, V. V.; Reneker, D. H. *Polymer* **1995**, *36*, 1791–1808.

Figure 1. UV−vis spectra of 0.05 mg/mL PTH solutions in TRIS buffers at pH = 7.5, 4, and 2.5 (A). The inset shows the optical appearance of the solutions in the optical cells. The corresponding fluorescence spectra at pH = 7.5, 4, and 2.5 (B).

deposition and exposure of the films to various pH conditions was done with a Bruker FTIR spectrometer Vertex 70 equipped with a narrow-band mercury cadmium telluride detector. The ATR surface was rectangular trapezoidal multiple reflection Si or Ge crystals of dimension 50 mm × 10 mm × 2 mm (Harrick Scientific) whose beam entrance and exit surfaces were cut at 45°. Interferograms were collected at 4 cm^{-1} resolution, and the number of averaged scans was 120. Each interferogram was corrected on the corresponding background, measured for the same ATR cell with the same D$_2$O buffer solution. The bare ATR crystal was used as a background. To eliminate overlap of the IR bands in the 1700−1500 cm^{-1} region with the strong water band, D$_2$O with 99.9% isotope content was utilized. Multilayer films of (PTH/polycation)$_5$ were deposited on a hydrophilic Si crystal in situ within the flow-through ATR-FTIR liquid cell: 0.5 mg/mL solutions of a polycation in 0.01 M TRIS buffer in D$_2$O were adsorbed onto the surface of the oxidized Si crystal at appropriate pH for 15 min, and after that the polymer solution was replaced by pure buffer solution in D$_2$O without polymer. A PTH was then deposited from 0.5 mg/mL solution, and the deposition cycle was repeated. The absorption peaks were analyzed with Galactic Grams/32 software as described elsewhere.[49]

Results and Discussion

pH-Dependent Properties of the PTH in Solution. Optical properties of PTH solution showed a dependence on the pH (Figure 1A). The UV−vis spectrum of the polymer at pH 7.5 possesses a peak with a maximum at a wavelength λ = 463 nm. When pH is decreased from slightly basic to slightly acidic, i.e., from pH 7.5 to pH 4, there is a minor blue shift to λ = 460 nm, which becomes more pronounced when the solution pH was further decreased to pH 2.5. The inset in Figure 1A illustrates the corresponding color transition from red to greenish for PTH in TRIS buffer solutions at different pH values.

The decrease in the absorption maximum along with the formation of an additional weak adsorption band around 800 nm is attributed to the oxidation of the thiophene rings from

(49) Izumrudov, V.; Kharlampieva, E.; Sukhishvili, S. A. *Biomacromolecules* **2005**, *6*, 1782–1788.
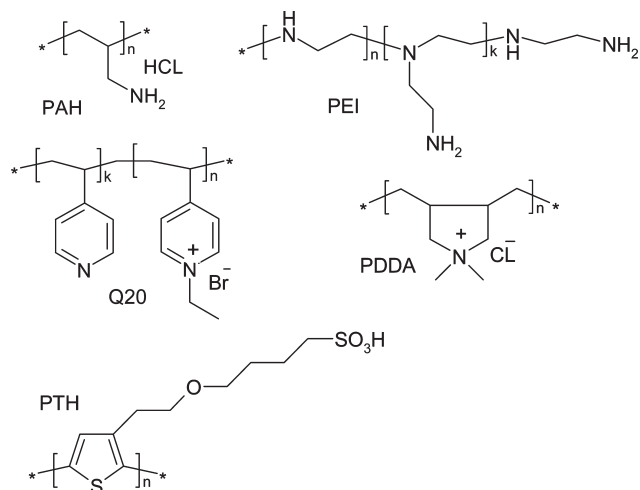
Figure 2. Chemical structures of poly(allylamine hydrochloride) (PAH), poly(ethylenimine) (PEI), poly(*N*-ethyl-4-pyridinium bromide) with 20% quaternization degree (Q20), poly(diallyldimethylammonium chloride) (PDDA) polycations used for LbL assembly with the water-soluble polyanion, and poly[2-(3-thienyl)ethyloxy-4-butylsulfonate] (PTH).

the acid-catalyzed photooxidation.[50] The greenish color of a solution is therefore caused by absorptions close to 400 nm and near 800 nm. Such dramatic change in color upon the acid protonation is accompanied by an oxidation of the polythiophenes known as a self-acid-doping.[51] Although PTH is a strong polyanion due to the presence of one sulfonate group per monomer unit, acid-induced oxidation of the polymer introduces positive charges in the thiophene backbone, thereby reducing the overall charge density of PTH.[51]

The fluorescence properties of PTH in aqueous solution follow the similar trend as light absorption discussed above. As seen from Figure 1B, the decrease in solution pH from 7.5 to 4 causes a shift of the fluorescence peak to a shorter wavelength from initial emission peak at 596 to 589 nm at pH = 4 and to 572 nm at pH = 2.5, which was accompanied by a drastic 30-fold decrease in almost quenched fluorescence of the polymer solution at pH = 2.5.

LbL Assembly of the PTH with Various Polycations. The chemical structures of the conjugated polymer and different polycations used in this work are shown in Figure 2. As clear from these structures, PTH can be assembled with the polycations through electrostatic interactions because of negative sulfonate groups present in a side chain of the conjugated polymer in contrast to positive groups in the counterparts. The polycations were chosen on the basis of several reasons. First, we wanted to explore the effects of a variable charge density on the SA-LbL with PTH and the pH-dependent properties of the produced films. This can be achieved by using permanently charged polycations with a different amount of charged groups at a certain pH, i.e., PDDA with one positive charge per monomer unit and Q20 with 20% of pyridinium groups at high pH. On the other hand, the balance of charges can be varied when weak polyelectrolytes are exposed to different pH conditions, which can also affect deposition and properties of the produced constructs. The functional groups in the selected weak polyelectrolytes, i.e., PAH, PEI, and Q20, have different pK_a values (pyridine or different types of amine groups) which allows a good control over the charge density, important for the exploration of pH-responsive properties. Also, considering that the structure of polyelectrolytes can
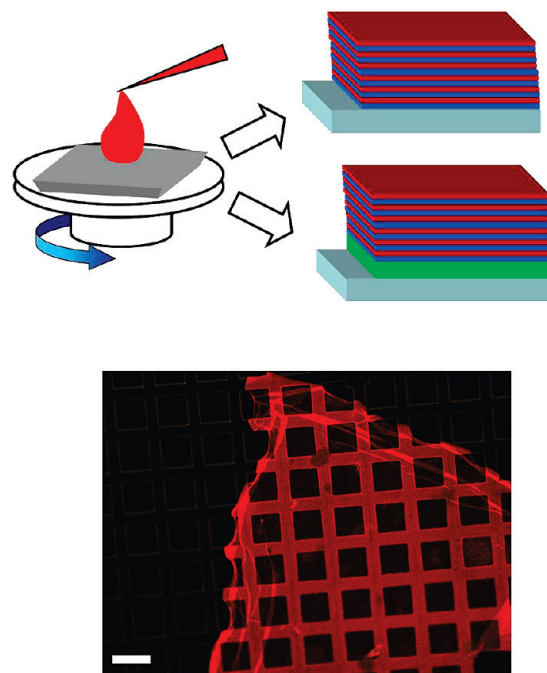

Figure 3. Top: spin-assisted LbL assembly of the conjugated polymer, PTH, with various polycations on bare silicon wafers (top) and on prelayers of (PAH/PSS)$_3$ or sacrificial layer of acetate cellulose. Bottom: a free-standing film of 20-bilayer (PDDA/PTH) assembled at pH 7.5 on a copper TEM grid; scale bar is 200 μm.

play an important role in the formation of the multilayers, branched PEI was selected.

The SA-LBL procedure applied in this study is schematically presented in Figure 3. It should be noted that even there are reports evidencing stratification of layered structures produced through SA-LbL, interpenetration between polycation and PTH layers to some extent might be possible.[41] Two types of films were prepared, first, directly assembled on bare silicon wafers or quartz slides, while in the case when free-standing films were required; a sacrificial layer of acetate cellulose was spin-cast and spun before the deposition of the PTH-containing multilayer (Figure 3, bottom).

Figure 4A demonstrates the growth of the films assembled at pH = 7.5 for different PTH/polycation systems monitored by ellipsometry. Figure 4B shows the LbL growth of the Q20/PTH films at pH = 7.5 as monitored by ATR-FTIR. One can see that the deposition of the polymers can be monitored by the absorption bands from Q20 (at 1648 and 1601 cm^{-1}) and PTH (at 1100 cm^{-1}) (see below for the bands assignments).

Our results show that all four systems can be successfully fabricated at high pH with the average thickness measured for the first 10 bilayers of 3.9, 3.2, 2.3, and 1.6 nm per a bilayer for Q20/PTH, PAH/PTH, PEI/PTH, and PDDA/PTH, respectively. However, Q20/PTH and PAH/PTH systems demonstrate the linear growth, while the PEI/PTH and PDDA/PTH films produced very thin layers for the first 4−6 bilayers. This can be explained by the template effect due to strong ionic interactions of brunched-PEI and PDDA with a highly charged surface of substrates at pH 7.5, which results in strongly stretched conformations of these polymers and consequently thin films. Indeed, silanol groups of silicon oxide surface utilized here are highly ionized at pH 7.5 because pK_0 and pK_a of surface silanol groups are 2−3 and 9.1−9.4, respectively.[52]

(50) Chayer, M.; Faid, K.; Leclerc, M. *Chem. Mater*. **1997**, *9*, 2902−2905.
(51) Chen, S. A.; Hua, M. Y. *Macromolecules* **1993**, *26*, 7108−7110.

(52) Sukhishvili, S. A.; Granick, S. *J. Chem. Phys*. **1998**, *109*, 6861−6868.
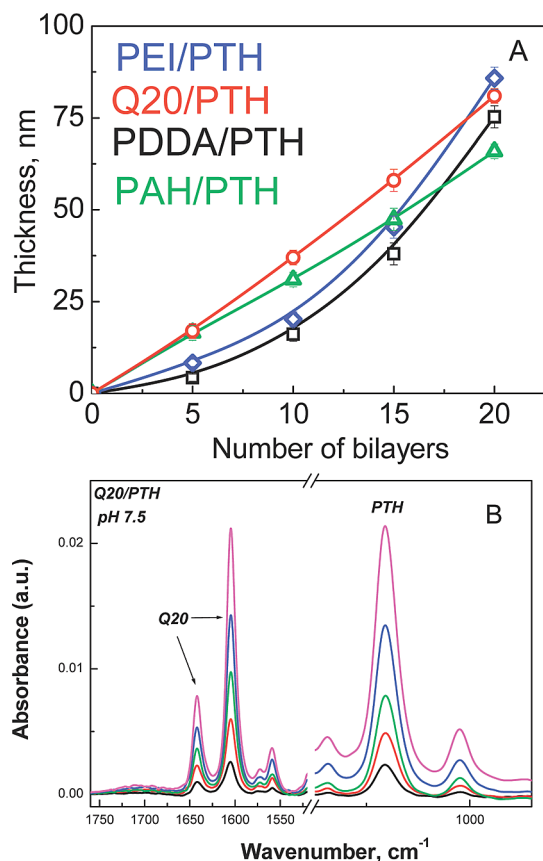
Figure 4. (A) LbL growth of PTH SA-LbL films assembled with PDDA (squares), Q20 (circles), PEI (diamonds), and PAH (triangles) at pH = 7.5. (B) LbL growth of Q20/PTH film followed by in situ ATR-FTIR. Bands centered at 1648 and 1601 cm^{-1} represent alkylated (ionized) and nonalkylated units of Q20. A peak at 1100 cm^{-1} corresponds to sulfonate groups of PTH.

When the assembly of the conjugated polymer with polycations was performed at pH = 4, only (Q20/PTH) and (PDDA/PTH) films could be formed (Figure 5A). Moreover, we observed a decrease in a bilayer thickness for (Q20/PTH) and (PDDA/PTH) systems with the average thickness values of 3.4 and 1.0 nm, respectively. These changes in the thickness of the (Q20/PTH) films can be caused by the appearance of additional positive charges in the polymer chain at pH 4 when ~25% of nonquaternized pyridinium groups become protonated (pK_a of quaternized poly(4-vinylpyridine) is 3.0−3.6).[53]

PAH/PTH films were the least robust and assembled with PTH only at pH = 7.5 when PAH charge density was the lowest (pK_a of PAH is around 8.8[54]). Our experimental observations on the SA-LbL growth (thicknesses) of the PTH films with the polycations used in this work correlate well with the estimated amounts of positively charged groups in PDDA, Q20, PEI, and PAH polycations present in solutions at pH = 7.5, 4, and 2.5 according to their pK_a values which are summarized in Table 1.

It has been observed that failure in LbL film assembly can occur during deposition of strongly charged polyelectrolytes due to competitive removal of the polymer chains into water-soluble complexes.[55] The decrease in the film thickness was observed when the charge density on polyelectrolyte was increased for both
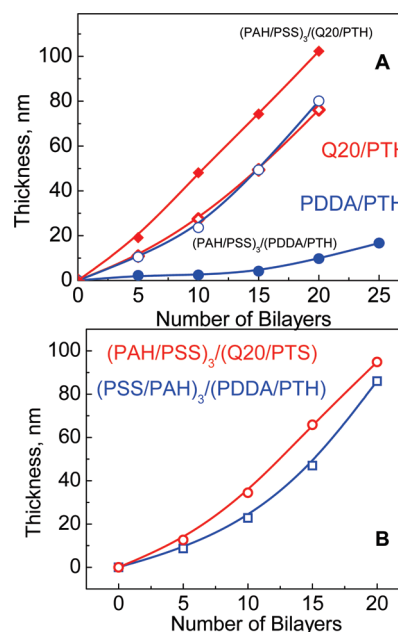

Figure 5. (A) SA-LbL growth of PTH assembled with PDDA (filled circles), Q20 (open squares) at pH 4 on bare Si wafers, and at pH = 4 on top of (PAH/PSS)$_3$ prelayers (open circles and filled squares, respectively). (B) LbL growth of PTH assembled with PDDA (squares) and Q20 (circles) at pH = 2.5 on top of (PAH/PSS)$_3$ prelayers.

strong and weak polyelectrolytes.[56,57] On the other hand, significant contribution to the LbL growth and stabilization of the multilayers can be due to nonelectrostatic (hydrophobic) interactions adding to the binding energy.[49,55] Clearly, the decrease in the deposition pH from 7.5 to 2.5 for our systems resulted in either formation of thinner films or inhibition of the multilayer formation for PEI/PTH and PAH/PTH films due to strongly increased charge density (>90%) (Table 1). These effects can be also explained by the reduced charge density of the PTH polymer at lower pH due to the acid protonation mentioned above. In this case the PTH behaves similarly to that of weak polyelectrolytes, such as poly(carboxylic acid)s, whose protonation at lower pH might inhibit the formation of ionic interactions with the charged counterparts.[58]

However, in the case of PDDA and Q20 polycations, the LbL film growth was still possible although with smaller thicknesses per a bilayer (4 nm vs 3.0 nm for Q20/PTH at pH 7.5 and 2.5, respectively, and 1.6 nm vs 1.0 nm for that for PDDA/PTH) which is probably due to the nonelectrostatic contributions to the stabilization of these films at low pH.

To eliminate a possible effect of a charged substrate on the growth of the films at lower pH values, we spin-cast three bilayers of (PAH/PSS) onto silicon substrates as prelayers for the films grown at pH = 4 and 2.5. Such pretreatment was generally favorable for the film deposition with an average increase in a bilayer thickness by almost 50% for Q20/PTH films and 70% for PDDA/PTH multilayers assembled at pH = 4 (5.0 nm/bL and 2.2 nm/bilayer, respectively) and pH = 2.5 (5.5 nm/bL and 2.2 nm/bL, respectively) (Figure 5A,B). However, PEI/PTH films were able to grow only when deposited on the prelayers at pH = 4 with an average thickness of 2.8 nm per a bilayer.

(53) Fujii, S.; Read, E. S.; Binks, B. P.; Armes, S. P. *Adv. Mater.* **2005**, *17*, 1014–1018.
(54) Choi, J.; Rubner, M. F. *Macromolecules* **2005**, *38*, 116–124.
(55) Sukhishvili, S. A.; Kharlampieva, E.; Izumrudov, V. *Macromolecules* **2006**, *39*, 8873–8881.

(56) Böhmer, M. R.; Heesterbeek, W. H. A.; Deratani, A.; Renard, E. *Colloids Surf., A* **1995**, *99*, 53–64.
(57) Glinel, K.; Moussa, A.; Jonas, A. M.; Laschewsky, A. *Langmuir* **2002**, *18*, 1408–1412.
(58) Kharlampieva, E.; Sukhishvili, S. A. *Langmuir* **2003**, *19*, 1235–1243.

Table 1. Estimated Amount of Positively Charges in PDDA, Q20, PEI, and PAH Polycations Present in Solutions at pH 7.5, pH 4, and pH 2.5 According to Their pK_a Values

		amount of groups able to carry positive charge, %		
polymer	pK_a	pH 7.5	pH 4	pH 2.5
PDDA	n/a	100	100	100
Q20	3.6−3.0[53,65,66]	20	∼60	>90
PEI	9.5 (primary), 7 (secondary), 3 (tertiary)[67]	∼38	∼88	>90
PAH	8.8[54]	∼75	>90	>90
PTH	1[a]	∼100	n/a	n/a

[a] Sulfonate groups have a pK_a < 1; however, pK_a increases to 5.6, when adsorbed on a polycation due to electrostatic interactions between anion−anion groups.[68]

Morphology of the PTH/Polycation Films. As has been previously discussed, the degree of ionization of the polyelectrolytes depends on the pH of the surrounding medium. The degree of ionization affects the proportion of free ionic binding sites and, consequently, the morphology of the polymer chains. Therefore, the thickness and roughness of the LbL films are strongly dependent on the pH of the polyelectrolyte solutions.[59] On the other hand, the degree of self-acid-oxidation of PTH can strongly affect the roughness of the produced films due to the conversion of the thiophene rings into more rigid quinine-like structures at lower pH values.[51] First, solutions of PTH at the pH values used during the assembly were examined for possible PTH aggregation upon pH lowering. For that, a drop of PTH solution at pH 7.5, 4, or 2.5 was deposited onto a Si wafer coated with a layer of PAH for better adhesion. AFM analysis did not reveal any pH-triggered nanoaggregation of PTH when pH was lowered from 7.5 to 4 and to pH = 2.5 (Figure 6). The average height of the spherical PTH domains observed in the AFM images kept the same, i.e., 2.4 ± 0.4, 2.3 ± 0.5, and 2.4 ± 0.5 nm for PTH solutions at pH 7.5, 4, and 2.5, respectively. AFM analysis of the PTH/polycation films constructed at pH 7.5 revealed high microroughness of the films (Figure 7). While relatively low for Q20/PTH (1.8 nm) and PDDA/PTH (2.2 nm) films (here and below measured at 1 × 1 μm^2 areas), the roughness values increased almost twice for PAH/PTH (3.3 nm) and PEI/PTH (3.7 nm) films with partial dewetting also observed.

Changes in the surface morphology of the films when the deposition pH was lowered from pH = 7.5 to 2.5 are presented in Figure 8. We observed a dramatic increase in the film roughness from 4.5 to 7.9 nm for (Q20/PTH)$_{10}$ films deposited at pH = 4 and 2.5, respectively (Figure 8, A1−A3). A similar trend was observed for another weak polyelectrolyte system, PEI/PTH, when the film roughness increased almost 5 times when deposition pH was lowered from pH 7.5 to pH 4 (Supporting Information, S2−S3). However, when strong polyelectrolyte, PDDA, was used, the film microroughness did not show any significant change with the rms roughness value of 1.8 nm at pH = 4 and 2.5 (Figure 8, B1−B3). The observed increase in microroughness can be attributed to weakened interactions between PTH and the polycations due to reduced charge density of PTH under lower pH conditions.[60]

Effect of the Polycation and the Deposition pH on the Optical Properties of the PTH/Polycation Films. Figure 9A depicts the UV−vis spectra of the (PTH/polycation)$_{20}$ films assembled on quartz slides at pH = 7.5. The spectrum of PDDA/PTH has an absorbance peak at 493 nm. The peak is blue-shifted to 475 or 441 nm when the polycation was exchanged to Q20 or to PEI, respectively (Figure 9A). The same trend is observed for pH 2.5 when Q20 was used instead of PDDA, and the

absorbance peak from the films shifted from 493 to 450 nm (Figure 9B). The decrease in deposition pH from 7.5 to 2.5 had almost no effect on the absorbance peak position for PDDA/PTH SA-LbL films; however, for Q20/PTH films there was a blue shift by 20 nm.

A similar effect of a polycation on optical properties of PTH films was observed for the films deposited at pH 4 when the absorbance peak shifted from 490 to 472 nm and to 449 nm with the Q20, PDDA, and PEI polycations, respectively (Figure 10). These results reflect planar-to-nonplanar conformational transitions of the polymeric backbone induced by the interactions of the PTH side chains with the studied polycations.[61]

Clearly, such changes in the peak absorbance can be realized not only just by changing a polycation, but by changing pH deposition conditions for the same PTH/polycation system (Figure 11). We limited this comparison to only two, i.e., Q20/PTH and PDDA/PTH, systems because they were capable of forming SA-LbL assembly with PTH at all three studied pHs. Unlike the Q20/PTH films, where the change in deposition pH leads to films with absorbances at different wavelengths (Figure 11A), PDDA/PTH results in films with different optical properties only if deposited either at pH = 7.5 or pH 4, with the same properties for those formed at pH = 7.5 and pH = 2.5 (Figure 11B).

pH-Dependent Properties of PTH/Polycation Films. We further studied the response of the assembled PTH/polycation films to pH variations. The LbL films on substrates were immersed in solutions at a certain pH for 15 min, and their thicknesses were monitored by ellipsometry. Similar experiments were performed in situ on the films using ATR-FTIR spectroscopy. Figure 12 demonstrates the pH stability of the films assembled with each of the four polycations at pH = 7.5. It shows that the Q20/PTH and PEI/PTH films changed their compositions when alternatively exposed to pH = 2.5 or pH = 7.5. After an initial decrease by ∼66%, the thickness of the films leveled out and did not further change with cycling pH.

For in situ using ATR-FTIR studies, the (Q20/PTH)$_5$ films were also constructed on Si crystal in a flow-through cell, and their pH-triggered thickness changes were monitored (Figure 13A). The important feature of this technique is its ability to detect individual components of the layered films as well as any compositional changes based on monitoring the selected functional groups. Figure 13A shows that the spectrum of the film at pH = 4 is similar to that at deposition pH = 7.5 and has three major absorbance bands: two bands associated with in-ring skeletal vibrations of pyridinium (at 1648 cm^{-1}) and pyridine (at 1601 cm^{-1}) rings and a band centered at 1100 cm^{-1} associated with the sulfonate groups.[62]

(59) Hiller, J.; Mendelsohn, J.; Rubner, M. *Nat. Mater.* **2002**, *1*, 59–63.
(60) Lukkari, J.; Viinikanoja, A.; Paukkunen, J.; Salomäki, M.; Janhonen, M.; Aäritalo, T.; Kankare, J. *Chem. Commun.* **2000**, 571–572.
(61) Faïd, K.; Leclerc, M. *J. Am. Chem. Soc.* **1998**, *120*, 5274–5278.
(62) Kharlampieva, E.; Izumrudov, V.; Sukhishvili, S. A. *Macromolecules* **2007**, *40*, 3663–3668.
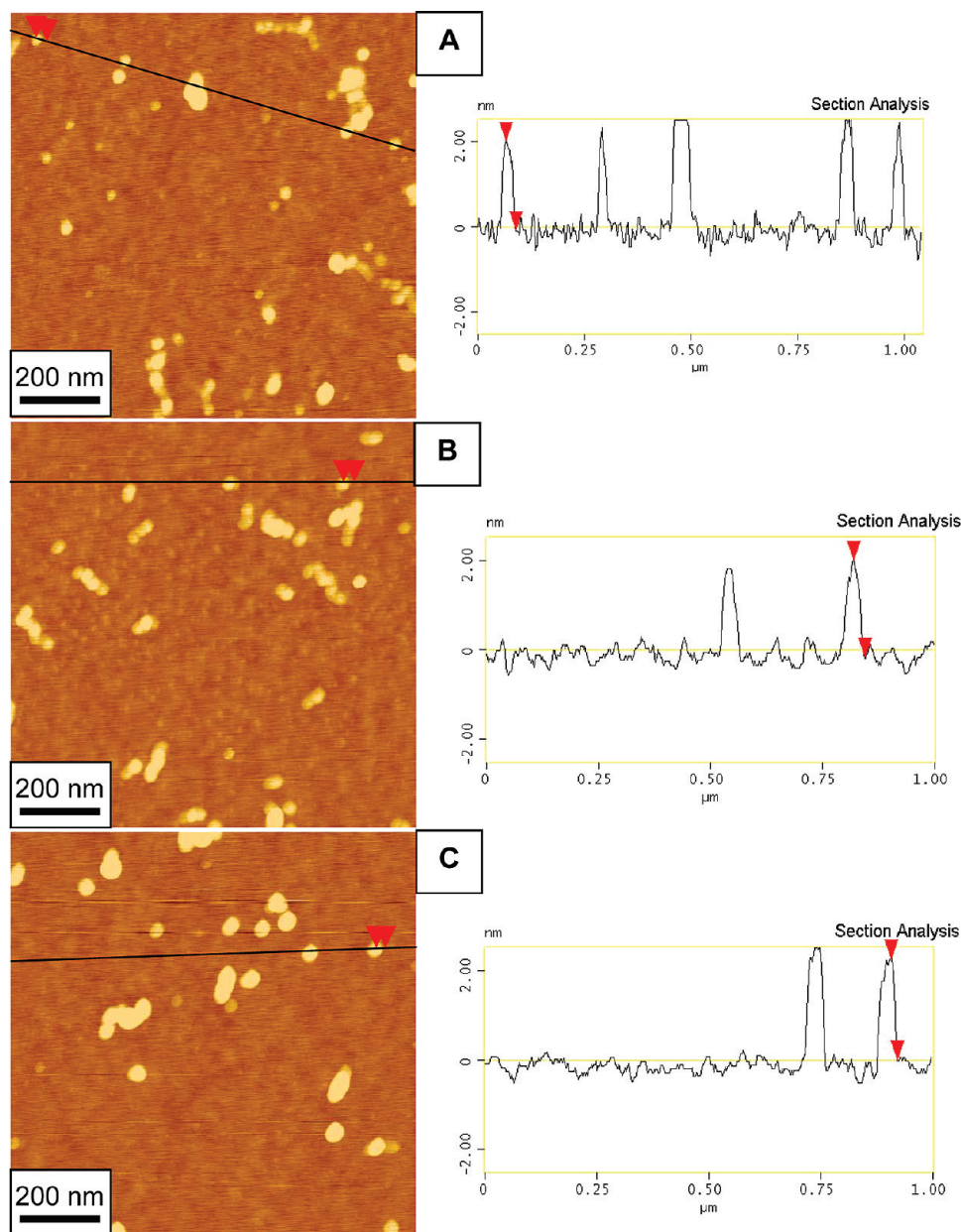
Figure 6. AFM images and section analyses of a PTH monolayer deposited from solution at pH 7.5 (A), at pH 4 (B), and at pH 2.5 (C). The *z*-range is 5 nm for all height images.

When the film was further exposed to pH = 2.5, we observed a partial release of the Q20 component from the film. Similar pH-triggered expulsion of one of the polymer component from the LbL film of Q20/poly(methacrylic acid) (PMAA) was reported earlier and attributed to pH-induced imbalance of negative to positive charges in the film as the driving force for the chain release.[63] However, in the present study the selective release of a polycation, Q20, occurred instead of a polyanion.[63] Also, the partial release of PTH (~10% of the initial amount deposited) occurred which is evident from the intensity decrease for the PTH band (Figure 13A). The release of a polycation was almost twice fast from the PEI/PTH films than in the Q20/PTH which agrees with the higher molecular weight of Q20 used in this study compared to that of PEI. The effect of molecular weight on release kinetics of PMAA from multilayer Q20/PMAA films was

earlier reported.[63] It has been shown that longer times are required for the release of longer polymer chains from the multilayer.

This effect of selective release of a polycation from the PTH-containing films was not possible when PTH was assembled with a strong polyelectrolyte, i.e., permanently charged polycation, PDDA (Figure 13B). There was a slight mass loss for the PDDA/PTH film when it was cycled between pH = 7.5 and pH = 2.5 (ellipsometry) with almost no changes observed in ATR-FTIR experiments for that cycled between pH 7.5 and pH 4. The Q20/PTH and PDDA/PTH assembled at lower pH = 2.5 had a constant thickness at both pH = 7.5 and 2.5 which is due the fact that the charge density in PTH was at its minimum at deposition pH = 2.5, and there was no charge imbalance when pH was changed to 7.5.

When the PEI/PTH and the Q20/PTH films were transferred from pH = 7.5 to 2.5, the pH-dependent decrease in fluorescence was detected (Figure 14A,B). In both cases there were

(63) Kharlampieva, E.; Ankner, J.; Rubinstein, M.; Sukhishvili, S. A. *Phys. Rev. Lett.* **2008**, *100*, 128303/1–128303/4.
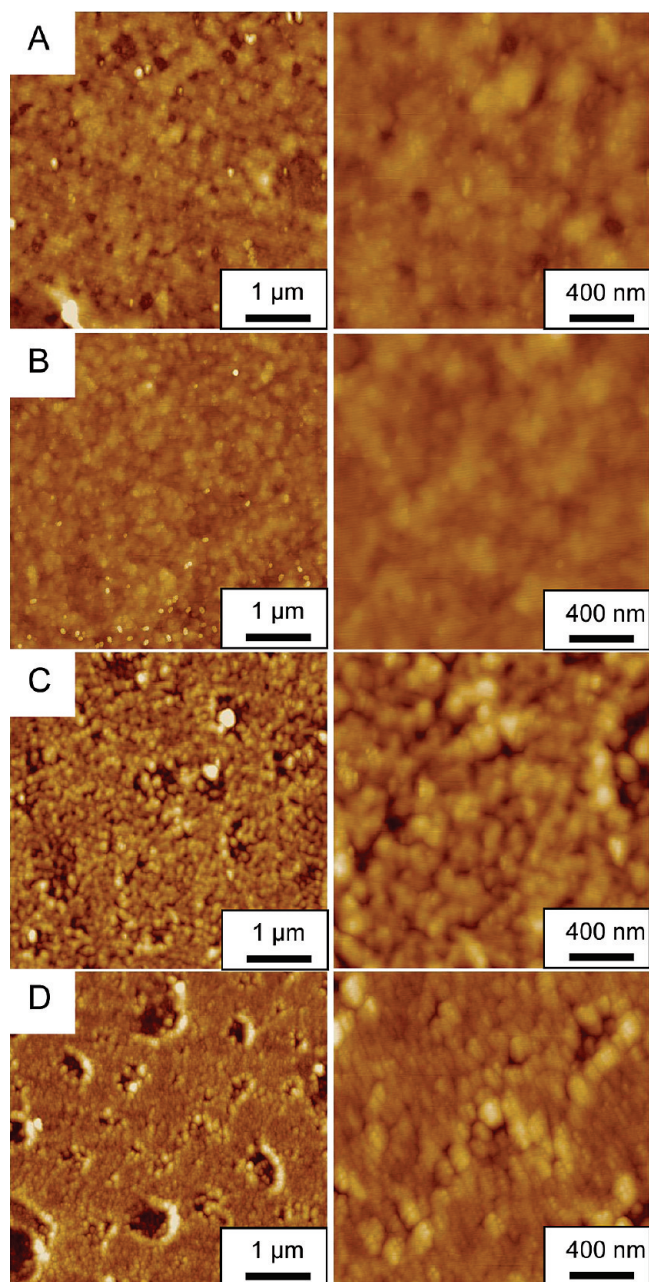
Figure 7. AFM images of 10-bilayer films of PDDA/PTH (A), Q20/PTH (B), PEI/PTH (C), and PAH/PTH (D) assembled via SA-LbL from solutions at pH = 7.5. The *z*-range is 50 nm for all images.

Figure 8. AFM images of a 10-bilayer Q20/PTH film deposited at pH = 7.5 (A1), pH = 4 (A2), pH = 2.5 (A3) and of a 10-bilayer PDDA/PTH film deposited at pH = 7.5 (B1), pH = 4 (B2), pH = 2.5 (B3); the *z*-range is 50 nm for all images.

Figure 9. Absorbance spectra of 20-bilayer films of PTH assembled with PEI, PAH, Q20, and PDDA from deposition solutions at pH = 7.5 (A) and pH = 2.5 (B).

fluorescence (FL) peak shifts to shorter wavelengths similar to that observed in the nonassembled conjugated polymer in solution (Figure 1A). Such quenching in fluorescence intensity can be attributed to additional acid-induced protonation of the amine or pyridine groups at lower pH which further leads to deconjugation and quenching of PTH within the SA-LbL membranes similarly to that of nonassembled PTH at this pH. When the film is transferred back to pH 7.5, deprotonation of the charged groups occurs and fluorescence is recovered. The change in fluorescence intensity was not completely reversible with partial (~50%) fluorescence recovery, which is in good agreement with the decrease in the membrane thicknesses confirmed by the ellipsometry and ATR-FTIR experiments. In contrast, PAH/PTH and PDDA/PTH films assembled at pH = 7.5 exhibited much lower fluorescence with almost 5-fold decrease in FL intensity
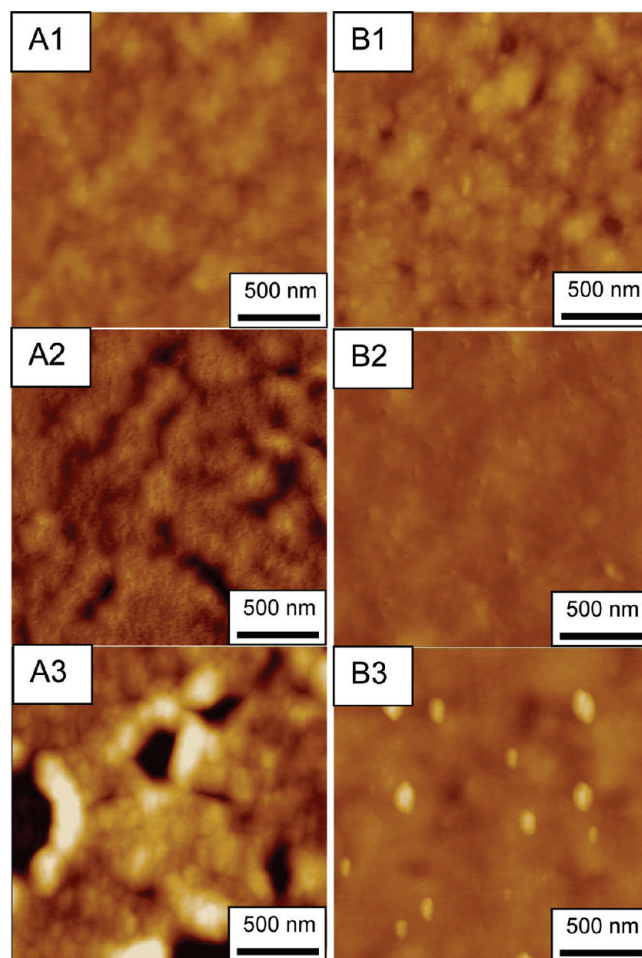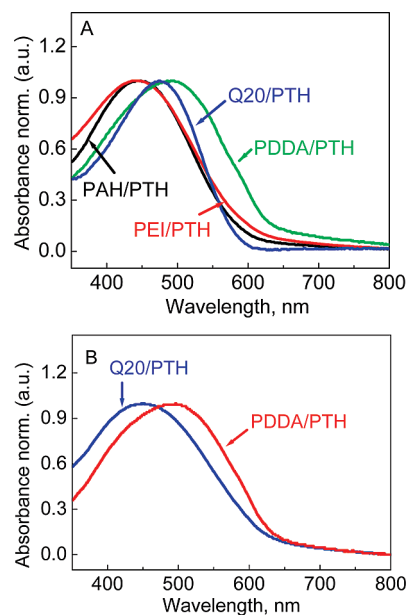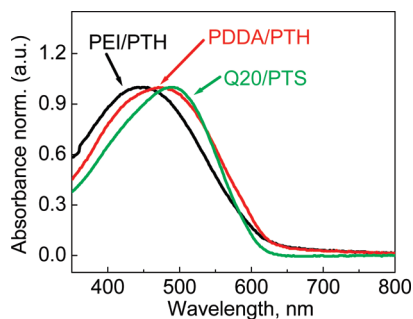
Figure 10. Absorbance spectra of 20-bilayer films of PTH SA-LbL assembled with PEI, PDDA, and Q20 polycations from deposition solutions at pH = 4.
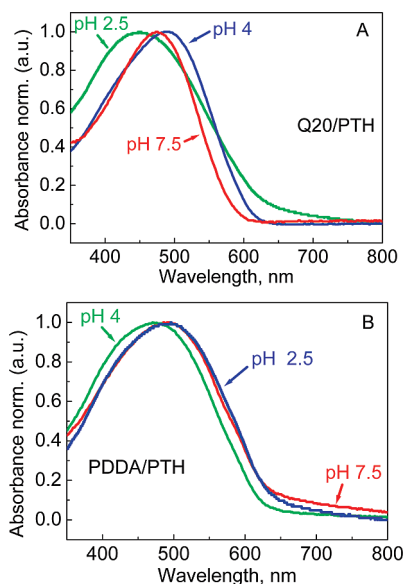

Figure 11. Absorbance spectra of 20-bilayer films of PTH SA-LbL assembled with Q20 (A) and PDDA (B) at pH = 2.5, at pH = 7.5, and at pH = 4.
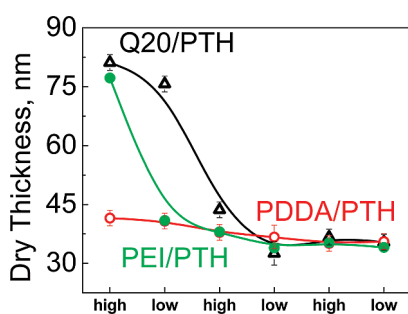

Figure 12. Thicknesses dependence of 20-bilayer PEI/PTH (filled circles), PDDA/PTH (open circles), and Q20/PTH (open triangles) films on exposure to pH = 7.5 (high) and pH = 2.5 (low).

compared to the PEI/PTH and Q20/PTH films (Figure 14C). The small change in the FL intensity for PDDA/PTH film upon a pH decrease from 7.5 to 2.5 can be explained by a slight decrease in thickness of these films (~15% vs 66% for the weak polyelectrolyte films).

Remarkably, when Q20/PTH and PDDA/PTH films were assembled at pH = 4, they exhibited almost no fluorescence, probably due to the conformations of the PTH chains under the
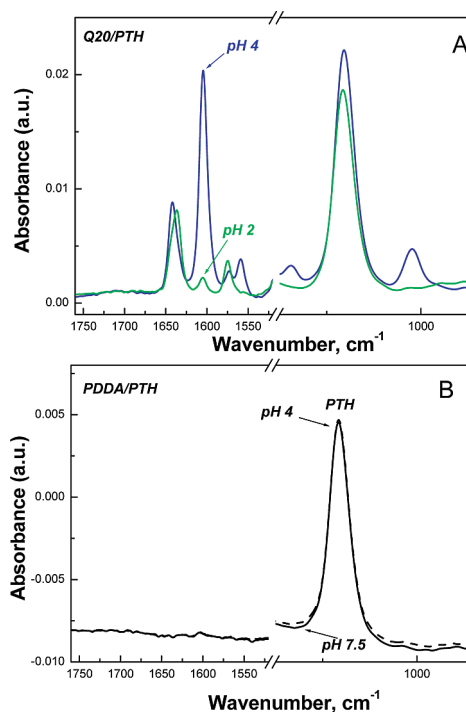

Figure 13. ATR-FTIR spectra of (Q20/PTH)₅ films deposited at pH = 7.5 and exposed to pH = 4 and pH = 2.5 (A). ATR-FTIR spectra of (PDDA/PTH)₅ films deposited at pH = 4 (solid curve) and exposed to pH = 7.5 (dashed curve) (B).
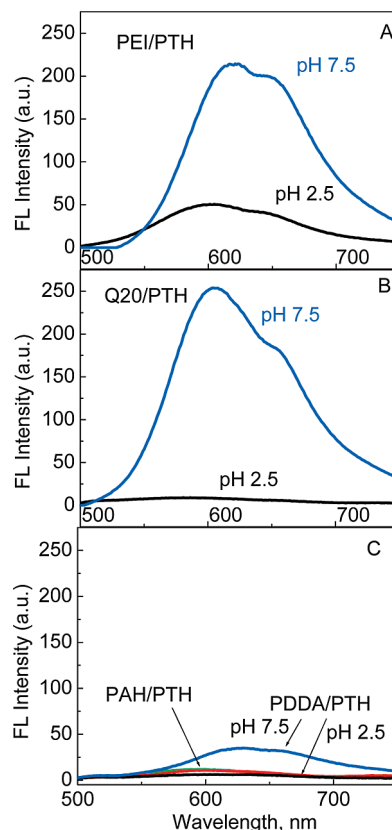

Figure 14. Fluorescence of quartz-tethered PEI/PTH (A), Q20/PTH (B), and PDDA/PTH (C) films deposited at pH = 7.5 and exposed to pH = 2.5 for 15 min. (C) Fluorescence of PAH/PTH films deposited at pH = 7.5 and exposed to pH = 2.5 are shown for comparison.
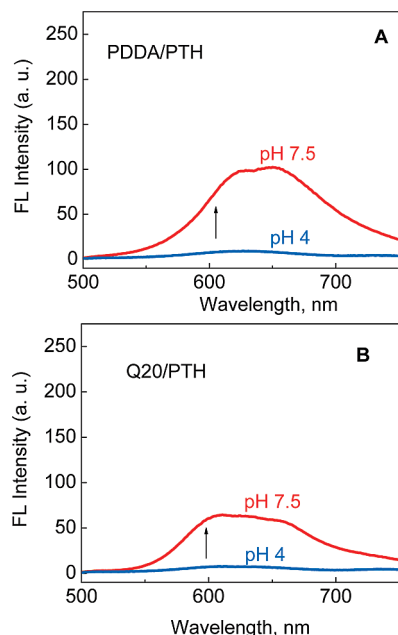
Figure 15. Fluorescence of quartz-deposited PDDA/PTH (A) and Q20/PTH (B) films deposited at pH = 4 and exposed to pH = 7.5 for 15 min.

assembly conditions with the reduced length of the conjugated segments[64] (Figure 15A,B). The exposure of these PDDA/PTH and Q20/PTH films to solutions at pH = 7.5 resulted in the increased fluorescence because of the restored flexibility of the PTH segments (Figure 15A,B). These results are promising for prospective development of robust and conformal coatings for optical monitoring and control of pH in confined and/or hard-to-reach spaces such as e.g. in closed environment of bioreactors without compromising their sterility requirements.

Finally, we tested the optical stability of the films after storage in the dark at ambient conditions. We found that the UV−vis intensity of the films could increase by almost 20% with the slight peak shift to longer wavelengths after 2 weeks of storage in air but was restored to the initial values after films were rehydrated in the solution with the appropriate pH values for 2 days (Supporting Information, S2). This effect can be further explored for preparation of sensing membranes for optical detection of trace amounts of water.

(64) Laurenti, M.; Löpez-Cabarcos, E.; García-Blanco, F.; Frick, B.; Rubio-Retama, J. *Langmuir* **2009**, *25*, 9579–9584.
(65) Fuoss, R. M.; Strauss, U. P. *J. Polym. Sci.* **1948**, *3*, 246–263.
(66) Kirsh, Yu. E.; Pavlova, N. R.; Kabanov, V. A. *Eur. Polym. J.* **1975**, *11*, 47–52.
(67) Tsuchida, E.; Nishikawa, J. *J. Polym. Sci., Polym. Chem. Ed.* **1976**, *14*, 1557–1560.
(68) Pauleau, Y. *Chemical Physics of Thin Film Deposition Processes for Micro- and Nano-Technologies*; Springer: Dordrecht, The Netherlands, 2002; p 384.

Conclusions

In summary, we demonstrated the SA-LbL assembly of the branched polyanionic conjugated polymer, PTH, with PAH, PEI, 20% quaternized poly(4-vinylpyridine), and PDDA polycations under different pH conditions. We showed that robust films with all these polycations can be produced at pH 7.5 and only with Q20 and PDDA at pH 4 and pH 2.5. Decrease in the deposition pH to 2.5 limits the PTH multilayer formation to Q20/PTH and PDDA/PTH films, possibly, due to reduced charge density in the sulfonate side chains due to self-acid-doping of the polymer at lower pH values. In contrast to the assembly of weak polyelectrolytes when lower charge density results in thicker films, demonstrated lowering charge density on PTH leads to less or no material deposited.

The surface morphology and optical properties of the LbL films assembled here, such as the absorbance maximum, can be tuned by changing a polycation component of the film and by varying the deposition pH for a particular PTH/polycation system. We show that fluorescence properties of the SA-LbL assembled Q20/PTH, PEI/PTH, and PDDA/PTH films are pH-dependent and exhibit the decrease in photoluminescent intensity when transferred from solution at pH = 7.5 to pH = 2.5 due to a pH-triggered selective release of the polycation component from the film. In case of Q20/PTH and PDDA/PTH films assembled at pH = 4, the fluorescence can be recovered upon pH changes to higher pH values. We suggest that the method of embedding pH-sensitive conjugated polymers into polymer matrices can be an effective means to combine unique pH-dependent optical properties of the conjugated polymers with adaptive behavior of ultra-thin membranes for easily handable responsive materials. Specifically, we suggest that the fluorescent LbL films fabricated here can render easily fabricated ultrathin membranes for optical sensing changes in the environmental conditions as robust wall coatings of bioreactor vessels for monitoring and control of pH in culture fluids in closed environment without compromising their sterility requirements or for optical pH sensing based on colorimetric sensing technology. Changes in fluorescent intensity in response to dehydration of the films can be further explored for preparation of sensing membranes for optical detection of trace amounts of water.

Supporting Information Available: Thickness data for films assembled through SA LbL method at various pH conditions; UV−vis spectra of the quartz-tethered films as fabricated from deposition solutions at pH 2.5, dried at ambient conditions for a week, and rehydrated at pH 2.5 for 2 days. This material is available free of charge via Internet at http://pubs.acs.org.